Morphological Studies of Polypropylene–Nanoclay Composites

Gopinath Mani,[1] Qinguo Fan,[1] Samuel C. Ugbolue,[1] Yiqi Yang[2]

[1]*Department of Textile Sciences, University of Massachusetts, Dartmouth, Massachusetts 02747-2300*
[2]*Department of Textiles, Clothing, and Design, University of Nebraska–Lincoln, Lincoln, Nebraska 68583-0802*

Received 17 November 2003; accepted 15 November 2004
DOI 10.1002/app.21750
Published online in Wiley InterScience (www.interscience.wiley.com).

ABSTRACT: Polypropylene–clay nanocomposites were prepared by a solution technique and a subsequent melt-mixing process. A titanate coupling agent was used to improve the compatibility of the nanoclay particles with the polypropylene. The dispersion of the nanoclay particles in polypropylene was studied with X-ray diffraction (XRD) and transmission electron microscopy (TEM). An increased *d*-spacing value of the clay particles in the nanocomposites was observed, and it was compared with the values of as-mined (pristine) and as-received (organophilic) clay particles. The number of intercalated layers in a single clay crystallite was determined to be 4, and the number was confirmed with XRD data and TEM images. On the basis of the Daumas–Herold model (which is widely used for graphite intercalation compounds), the stage 2 and stage 3 structures of montmorillonite particles in polypropylene were recommended. A study on the stage structure suggested a way of determining the presence of polymer molecules in the clay galleries. The results confirmed the existence of single-layered platelets with improved dispersion in polypropylene. © 2005 Wiley Periodicals, Inc. J Appl Polym Sci 97: 218–226, 2005

Key words: clay; morphology; nanocomposites; poly(propylene) (PP)

INTRODUCTION

The term *nanocomposite* describes a two-phase material in which one of the phases is dispersed in the second one at a nanometer (10^{-9} m) level. This term is commonly used in two distinct areas of materials science: polymers and ceramics. Polymer nanocomposites are an emerging class of mineral-filled plastics that contain relatively small amounts (usually <10%) of nanometer-sized inorganic particles.

Two major findings in the field of polymer nanocomposites began the study of these materials. First, Toyota researchers[1] reported nylon nanocomposites, for which moderate inorganic loadings resulted in concurrent and remarkable enhancements of the thermal and mechanical properties. Second, Giannelis[2] demonstrated the possibility of melt-mixing polymers and clays without organic solvents. Since then, the high promise of industrial applications has motivated vigorous research, which has revealed concurrent dramatic enhancements of many material properties by the nanodispersion of inorganic silicate layers.[1,2]

Clay minerals are phyllosilicates.[3] The principal building elements of clay minerals are two-dimensional arrays of silicon–oxygen tetrahedra and two-dimensional arrays of aluminum– or magnesium–oxygen–hydroxyl octahedra. Clay minerals are broadly classified into two types: 1:1 clays (one tetrahedral sheet is present for one octahedral sheet) and 2:1 clays (two tetrahedral sheets are present for one octahedral sheet). The 2:1 clay minerals are further subdivided into smectites, micas, vermiculites, and pyrophyllites.[3,4] Montmorillonite, a clay mineral that is widely used in the preparation of polymer nanocomposites, is classified as a smectite.

The structure of montmorillonite is derived from pyrophyllite by the substitution of certain atoms for other atoms.[4] In the tetrahedral sheet, tetravalent Si is sometimes partly replaced by trivalent Al. In the octahedral sheet, divalent Mg replaces trivalent Al without filling the third vacant octahedral position completely. In many types of minerals, an atom of lower positive valence replaces one of higher valence, and this results in a deficit of positive charge (i.e., excess negative charge). This excess negative charge is compensated by the adsorption of cations, which are too large to be accommodated in the interior of the crystal. In the presence of water, the compensating cations on the layer surfaces may be easily exchanged by other cations, which are called exchangeable cations. The total concentration of these cations can be determined analytically. This concentration (mequiv/100 g of dry clay) is called

Correspondence to: Q. Fan.
Contract grant sponsor: National Textile Center.

the cation-exchange capacity (CEC) or base-exchange capacity of the clay.[4]

The formula of a typical montmorillonite with a CEC of 70 mequiv/100 g is as follows:

$$((Si_{3\cdot88}Al_{0\cdot12})^{IV}(Al_{1\cdot64}Fe^{3}_{0\cdot05}Mg_{0\cdot36})^{VIII}O_{10}(OH)_2)_2$$
$$\Big|$$
$$M_{0\cdot67}$$

where M represents a monovalent exchangeable cation and the superscripts IV and VIII refer to tetrahedral and octahedral coordination, respectively.[4,5]

Montmorillonite particles are agglomerated within a distance of approximately 3.5 Å.[5] A surface treatment reduces particle–particle attraction, and this promotes an expansion of the distance (gallery) beyond 20 Å.[6] At this distance, the particles can be separated further either by the adsorption of monomer into the gallery before polymerization or, for a high polymer, by the use of a shearing force with a mixer or extruder.[7] Usually, the length and breadth of the clay particles range from 1.5 μm to a few tenths of a micrometer; however, the thickness is extraordinarily small, measuring only a few nanometers. These dimensions result in high average aspect ratios of 200–500.[3–8] Because of the hydrophilicity of the clay, most polymer–clay nanocomposites require the surface modification of clay to make the clay compatible with an organic polymer.

A promising way of synthesizing polymer nanocomposites is the intercalation of polymers in layered inorganic clay particles. The structure and properties of the resulting nanostructure can be altered by the control of subtle polymer–clay interactions.[9–11] Beyond the conventional approach, in which the polymer and clay particles remain immiscible, two types of hybrids are possible: intercalation and exfoliation. Intercalation is a state in which the extended polymer chains are present between the clay layers, and this results in a multilayered structure with alternating polymer and inorganic layers and a repeated distance of a few nanometers. Exfoliation is the state in which the silicate layers are completely separated and dispersed in a continuous polymer matrix.

A great deal of attention has been paid to the preparation of graphite intercalation compounds (GICs),[12,13] which are formed by the insertion of atomic or molecular layers of guest chemical species (intercalants) between layers of a host material. X-ray diffraction (XRD) measurements of GICs can be used to show periodic stacking structures.[13] According to the Daumas–Herold model,[13] when intercalants (guest species) exist between every n layer and $n + 1$ layer of the graphite (host), the periodically stacked structure is called a stage n structure.

The fine and homogeneous dispersion of nanoparticles throughout the polymer matrix is the key to developing a high-quality nanocomposite. Most of the property improvements of nanocomposites are generally believed to be dependent on the homogeneous and uniform dispersion of nanoparticles in the polymer matrix.

EXPERIMENTAL

Materials and instruments

Cloisite 15A (C-15A; Southern Clay Products, Inc., Gonzales, TX) was the organophilic montmorillonite clay used in this study. Isotactic polypropylene (PP) pellets (Phillips Sumika Polypropylene Co., The Woodlands, TX), xylene (Pharmco Products, Inc., Brookfield, CT), and titanate coupling agent Ken-React Lica 12 [i.e., titanium IV neoalkoxy tris(diisooctyl)phosphato-O; Kenrich Petrochemicals, Bayonne, NJ] were used. A CPX 750 ultrasonic processor (Cole-Parmer Instruments, Vernon Hills, IL) and a plasticorder melt mixer (Brabender, Hackenshack, NJ) were used for the preparation of the nanocomposites. A laboratory press (Carver, Inc., Wabash, IN) was used to make the nanocomposite films. An RU 300 X-ray diffractometer (with a Rigaku 18-kW rotating-anode X-ray generator, The Woodlands, TX) and a high-resolution transmission electron microscope (model 2010F, JEOL, Peabody, MA) were used to characterize the nanocomposites.

Methods

Preparation of the nanocomposites

PP nanocomposites were prepared with a combination of solution techniques and melt mixing. C-15A (5% on the weight of the polymer) was dispersed in xylene and ultrasonicated for 1 h. The ultrasonication parameters were a 90% amplitude, an 8-s pulse on, and a 4-s pulse off. The titanate coupling agent was added to the xylene/C-15A mixture, and then ultrasonication was continued for 15 min more. PP pellets were then added and dissolved in the xylene mixture. The mixture was heated to 170°C under ultrasonication, and the preparation of the composites was finished by the evaporation of xylene. Afterwards, the prepared nanocomposites were mechanically broken and mixed well in a Brabender plasticorder melt mixer. The variable parameters used in the mixer were screw speeds of 35 and 70 rpm for times of 30 min and 2 h at 170°C. Nanocomposite films 400 μm thick were prepared with the Carver laboratory press afterwards.

Characterization of the nanocomposites

Wide-angle X-ray scattering was conducted at the ambient temperature on a Rigaku rotating-anode diffrac-

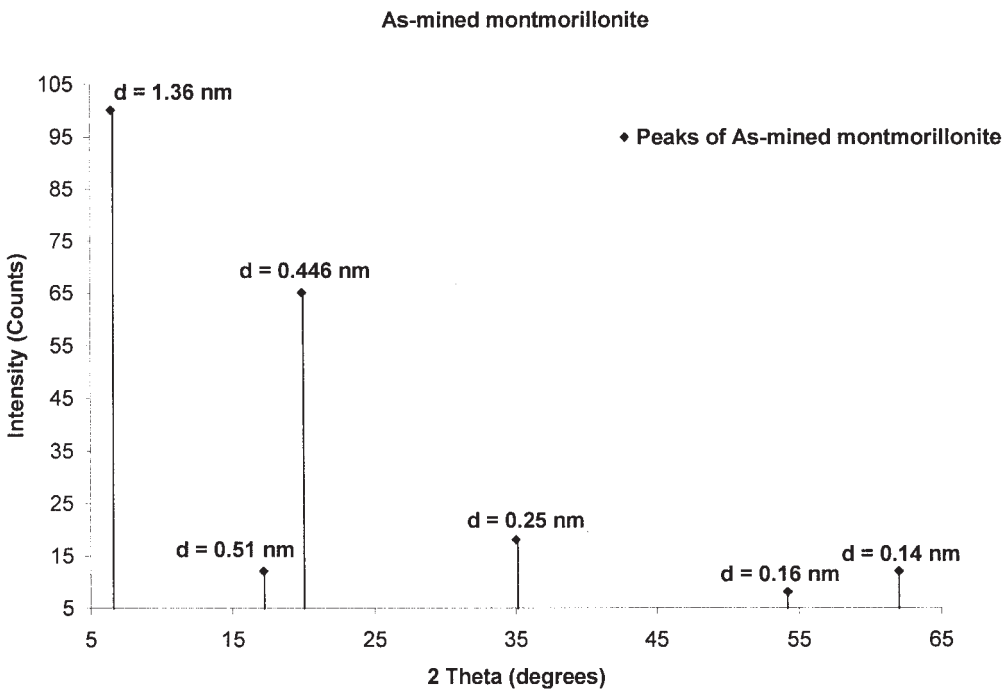

Figure 1 Peaks and *d*-spacings of as-mined montmorillonite clay particles.

tometer with Cu Kα radiation with a wavelength of 1.54 Å. The accelerating voltage was 60 kV. The montmorillonite clay particles were studied as powders, and the nanocomposites were studied as 400-μm thin films. A JEOL 2010F high-resolution transmission electron microscope, operated at 200 kV, with a point resolution of 1.9 Å and a lattice resolution of 1.4 Å was used to observe the physical state of the clay particles in the nanocomposites. For transmission electron microscopy (TEM) sample preparation, a diamond blade was used to scratch small specimen pieces from the bulk sample. These small pieces were then ground in an agate mortar with acetone. The acetone suspension was then pipetted onto a carbon-coated Cu grid. The prepared samples were used for TEM observations.

The characterization of the nanocomposite films prepared with a mixer running at 70 rpm for 2 h at 170°C showed increased *d*-spacing and a large number of single-layered exfoliated platelets in comparison with the films prepared at 35 rpm for 30 min. Therefore, the results obtained for the nanocomposites prepared at 70 rpm for 2 h were considered most appropriate for further analysis.

RESULTS AND DISCUSSION

The quaternary ammonium ion used for the organic modification of clay particles is unstable at a higher processing temperature (ca. 170°C), and this might cause a reversible reaction in which a clay's organophilicity turns into hydrophilicity.[14] However, the formation of an immiscible polymer–clay composite is avoided because of the xylene treatment, which retains the organophilic nature of the clay particles[4,6] until the composite is formed. Also, the difficulty of dispersing clay particles into the PP matrix can be minimized with xylene. However, the shear force produced by the melt mixer is considered to be an efficient source for exfoliating the clay platelets.[15–17] Thus, significant advantages are achieved by the combination of solution and melt-blending techniques for obtaining an improved dispersion of nanoparticles in the polymer.

XRD studies

As-mined montmorillonite clay particles (pristine), as-received nanoclay particles (C-15A), and nanocomposite films were characterized with XRD to determine the basal spacing of the fillers through the intercalation of polymer between the clay layers. Initially, the diffraction peaks and *d*-spacings of the as-mined montmorillonite particles were observed. The peaks of the as-mined montmorillonite clay particles occurred at 2θ values of 6.494, 17.170, 19.891, 35.022, 54.231, and 62.027° with *d*-spacings of 1.36, 0.51, 0.446, 0.25, 0.16, and 0.14 nm, respectively (Fig. 1).

To determine the change in the basal spacing, a d_{001} value of 1.36 nm at the (001) diffraction peak 2θ = 6.494° for the as-mined particles was compared with the corresponding values of C-15A and C-15A in nanocomposites. The (001) peak at 6.494° of the as-

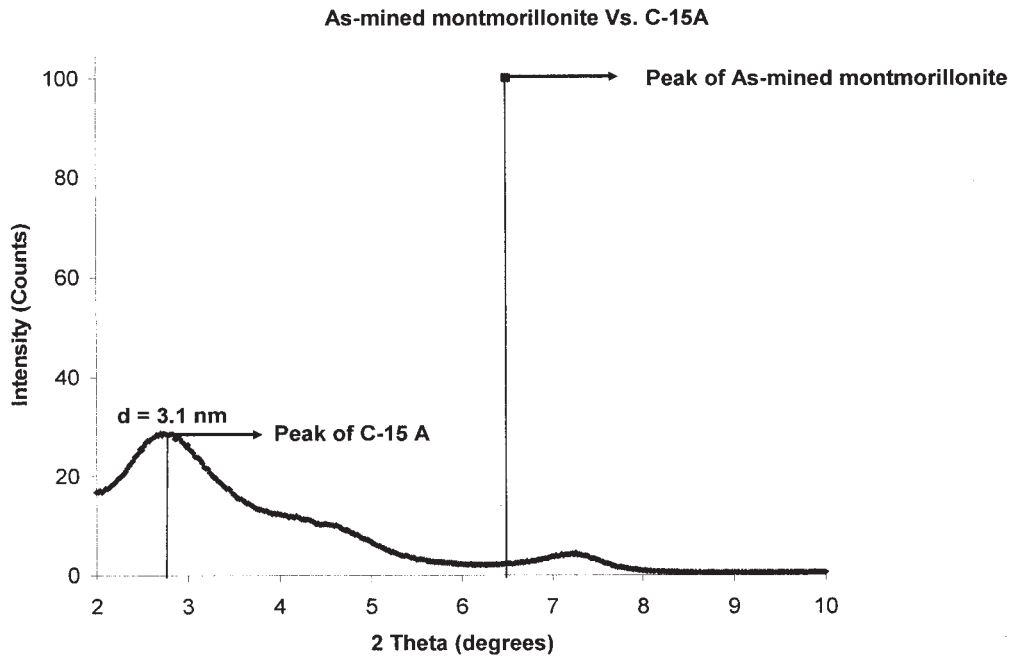

Figure 2 Peaks and *d*-spacings of C-15A and as-mined montmorillonite.

mined montmorillonite shifted to 2.760° in C-15A with a corresponding increase in the *d*-spacing from 1.36 to 3.1 nm (Fig. 2).

The increase in the interlayer spacing of C-15A was attributed to the surfactant used. Onium ion modification is essential for making the clay particles organophilic and also for increasing their *d*-spacing. Figure 3 shows the structure of the cationic surfactant, dimethyl dihydrogenated tallow quaternary ammonium ion. The increased *d*-spacing (Fig. 2) depends on the structure and quantity of the surfactants as well as the way in which the clay is modified.

Figure 4 shows that the (001) peak of C-15A at 2.760° shifted toward the left side with an increased *d*-spacing of 0.551 nm in the nanocomposites. The increased *d*-spacing might be attributable to PP molecules (the intercalants). According to intercalation theories,[13] *d*-spacing cannot be increased and sustained unless a secondary compound is present.

XRD plots for isotactic PP are shown in Figures 5 and 6. No peaks occurred between 2θ values of 2–10°, and this demonstrates that the (001) peak observed at $2\theta = 2.4°$ in Figure 4 represents that of the clay particles.

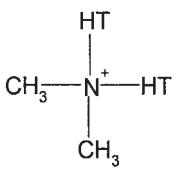

Figure 3 Structure of the surfactant used in C-15A (HT = hydrogenated tallow).

The *d*-spacing of 3.651 nm in the nanocomposites might be attributed to the presence of PP molecules. It can be concluded that during the formation of the nanocomposites, the PP molecules enter the galleries of the clay particles. It seems unlikely that either xylene or the coupling agent molecules will be found within the nanocomposites once they are duly processed. The reason for this lies in the fact that the boiling points of xylene and coupling agents are lower (135 and 105°C, respectively) than the composite processing temperature (170°C).

The dimension of a polymer most often used in discussing its configurations is the distance r between the ends of the chain. The appropriate average value of r is the root mean square ($\overline{r^2}^{1/2}$). The important measure of molecular size is the root-mean-square distance of the elements of the chain from its center of gravity ($\overline{s^2}^{1/2}$), which is the radius of gyration of the molecule. $\overline{r^2}^{1/2}$ and $\overline{s^2}^{1/2}$ are related as follows:[21]

$$\overline{s^2}^{1/2} = \left(\frac{\overline{r^2}}{6}\right)^{\frac{1}{2}} \tag{1}$$

$\overline{r^2}^{1/2}$ can be determined as follows:

$$\overline{r^2}^{1/2} = l \times n^{\frac{1}{2}} \tag{2}$$

where l is the average length of the segment and n is the number of segments in the chain. The values of l

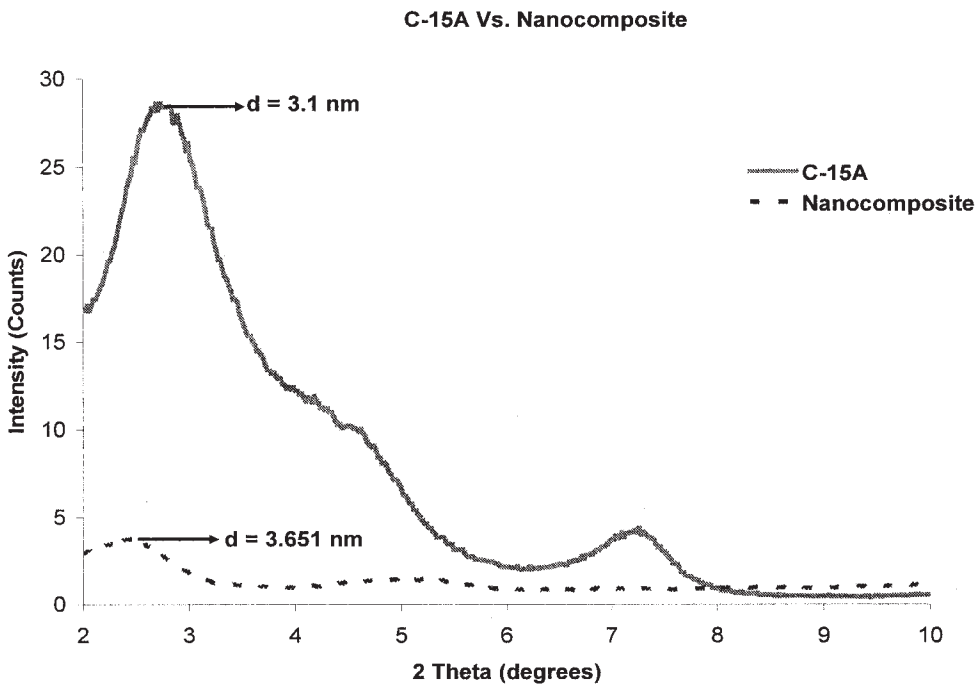

Figure 4 XRD plot for C-15A and PP nanocomposites (5% filler).

and n for PP were calculated. l was 1.54 Å (C—C is the only bond present in the backbone of a PP molecule, the bond length of which is 1.54 Å), and n was[18,19]

$$n = [(\text{Degree of polymerization} \times 2) - 1] \quad (3)$$

for PP. Given that the number-average molecular weight (M_n) of PP was 80,000 and the molecular weight of a repeating unit of PP was 42, the degree of polymerization was equal to M_n of PP divided by the molecular weight of a repeating unit of PP (i.e.,

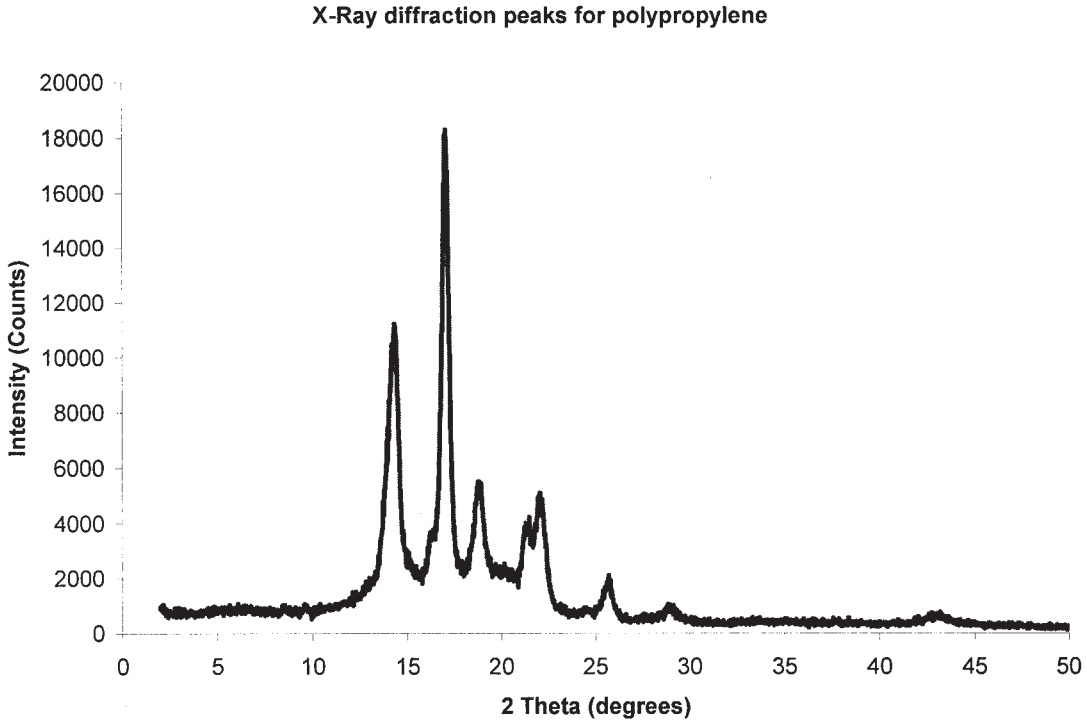

Figure 5 XRD plot for isotactic PP.

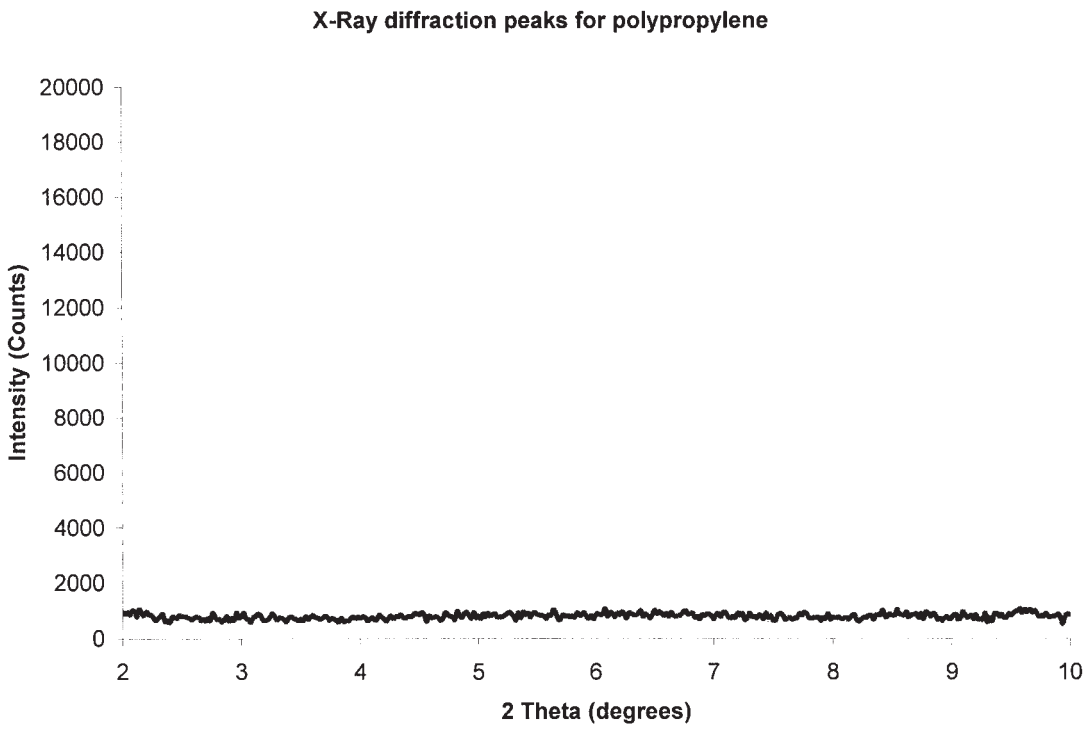

Figure 6 XRD plot for isotactic PP at 2θ = 2–10°.

80,000/42 = 1904.76). By substituting 1904.76, the degree of polymerization, into eq. (3), we found that n was 3808.5, and so $\overline{r^2}^{1/2}$ was 9.5 nm. Thus, $\overline{s^2}^{1/2}$ was 3.88. Similarly, the values of $\overline{s^2}^{1/2}$ for the corresponding M_n values of PP were calculated (Fig. 7).

The d-spacing of C-15A, as determined from XRD, was 3.1 nm (Fig. 2). Thus, the PP molecules, the molecular weight of which was less than 51,056, had a radius of gyration that was less than 3.1 nm (Fig. 7). This shows the good possibility that the PP molecules of $M_n < 51{,}056$ could enter the clay galleries with a d-spacing of 3.1 nm.

Modeling of the stage structure of the nanocomposites

When polymer molecules exist in a gallery, the d-spacing value is usually high. On the contrary, when the molecules do not exist in a gallery, the d-spacing

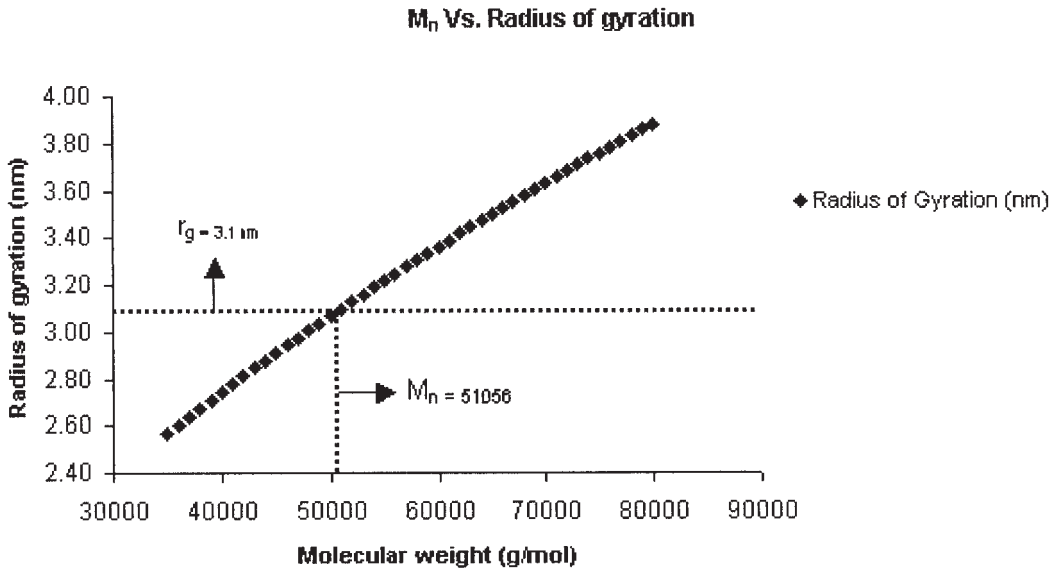

Figure 7 Graphical plot of the molecular weight versus the radius of gyration for PP molecules.

TABLE I
Number of Clay Layers Calculated for C-15A and the Nanocomposites

Material	Crystallite thickness (nm)	*d*-spacing (nm)	Number of clay layers (crystallite thickness/*d*-spacing)
C-15A	12	3.100	4
Nanocomposites	13	3.651	3–4

value is expected to be lower. The *d*-spacing of 3.651 nm is actually the average value of the different *d*-spacings between the platelets of a clay crystallite. According to the Daumas–Herold model,[13] the stage structure of C-15A in the nanocomposites was determined as follows.

The number of platelets in a clay crystallite can be calculated as follows:

$$\text{Number of platelets} = \text{Crystallite thickness}/d\text{-spacing} \quad (4)$$

The crystallite thickness was calculated with the software associated with the diffractometer used. This involved fitting a profile to the diffraction pattern. In this case, the strains were calculated, and the instrumental broadening was used. Several peaks were used, and a least-square fit was applied to the results to obtain an average size. The crystallite thicknesses of C-15A and C-15A in the nanocomposites were calculated to be 12 and 13 nm, respectively.

With the determined *d*-spacing and crystallite thickness, the number of layers calculated by eq. (1) is almost equal to 4 (Table I), and this has led us to assume that there are three gallery spaces present in a clay crystallite.

The increased *d*-spacing of 3.651 nm in the clay crystallites of the nanocomposites is marginally less than the calculated radius of gyration, 3.87 nm. Hence, the probability of the presence of PP molecules in more than one gallery is extremely low because it is unlikely for the polymer molecules to be highly oriented and exist as single molecules in two gallery spaces. For this reason, the clay particles in the nanocomposites are considered to form a stage 2 structure according to the Daumas–Harold model.

The stage 2 structure of the clay particles indicates that the intercalants (i.e., PP molecules) exist between every second and third layer of the clay platelets. Thus, it is concluded that out of the three gallery spaces, the PP molecules can exist in only one gallery space.

In the schematic shown in Figure 8, the intercalants (PP molecules) enter gallery 2 and gallery 3 to represent the corresponding stage structures 2 and 3 [Fig. 8(a,b)]. The layers drawn with solid lines are real, and the virtual layers are drawn with dotted lines. The virtual layers and virtual galleries are the imaginary layers and galleries. They are inserted for a better understanding of the intercalation model. Therefore, the real galleries are 1, 2, and 3, and the virtual galleries are 1′, 2′, and 3′. In both stage 2 and 3 structures, the second possibility of the presence of polymer molecules lies in the virtual galleries. Therefore, it is concluded that there is a very high probability of the PP molecules being present in only one of the gallery spaces.

TEM images and their interpretation

Because of the large number of defects (surface pores, fissures, cracks, and voids) inherited from the mined clay particles, the intercalation stability of the clay particles is very low in comparison with that of highly stable graphite intercalated compounds. When the intercalants enter the clay galleries, the strain becomes excessive and ultimately results in exfoliation, as shown in the TEM images.

Several TEM images were taken at various magnifications to characterize the nanocomposites. Six TEM images were taken for each of the nanocomposite samples. We observed fully exfoliated morphologies in some of the TEM images of the prepared nanocomposites (Figs. 9–11). The majority of the nanocomposites were filled with many exfoliated platelets. They could be defined as intercalated with XRD because there was an observed increase in the *d*-spacing in comparison with the original clay *d*-spacing.

A TEM image (Fig. 9) of the nanocomposites clearly indicate that the clay layers are not strictly flat: they are wrinkled, bent, or oriented toward one direction, and this can be considered a good sign for extruding a nanocomposite fiber. Three zones of a high-resolution TEM image (Fig. 9) have been enlarged to show the existence of intercalated tactoids. The number of layers in the intercalated tactoids was found to be around 4, and this supports our assumption based on the XRD results. Although all the TEM images greatly favor a significant existence of single-layered platelets (exfoliated), some images (Figs. 9, 12, and 13) present intercalated/exfoliated nanocomposites. These images confirm the existence of intercalated tactoids and exfoliated platelets. The images (Figs. 10 and 11) show that the platelets are exfoliated completely and are uniformly dispersed in the polymer matrix.

All the circles in Figure 9(a–c) indicate the presence of intercalated tactoids with four to five layers.

It is very interesting to observe the presence of intercalated tactoids with four layers each in the TEM images [Fig. 9(a–c)], and this greatly supports the XRD results (Table I). Also, the 20-nm scale can be

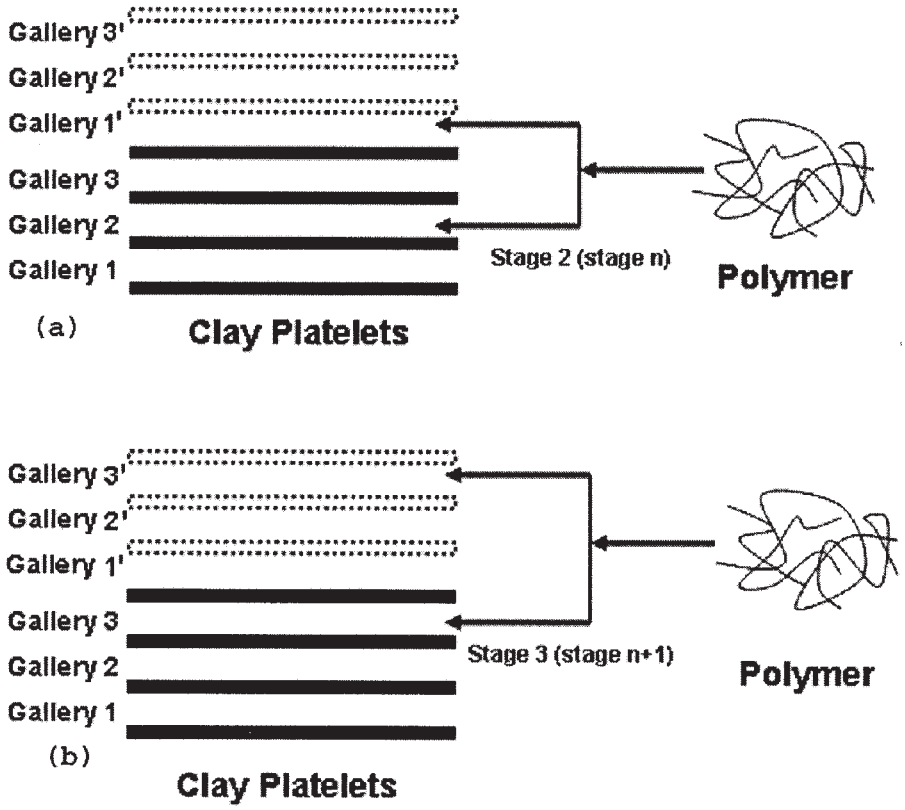

Figure 8 (a) Stage 2 structure (stage n) and (b) stage 3 structure (stage $n + 1$), respectively.

placed over the intercalated tactoid images (Fig. 9) to strongly support the XRD results on the number of layers (four) and the crystallite thickness (13 nm) of the clay particles in the nanocomposites.

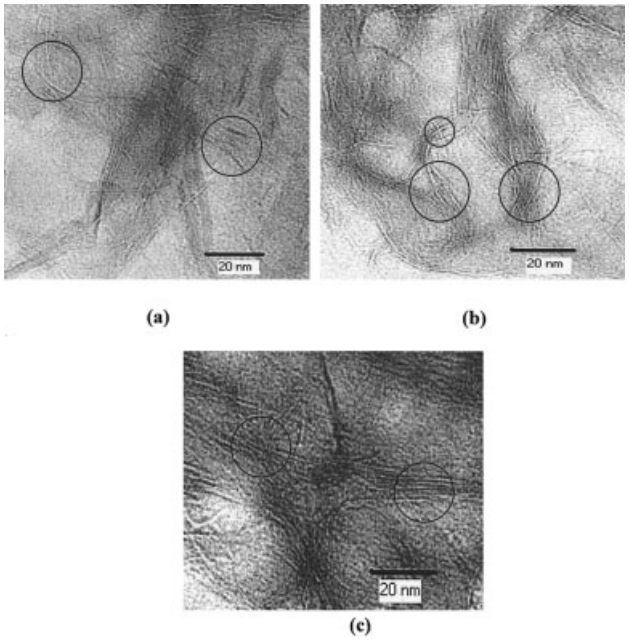

Figure 9 High-resolution TEM images of a C-15A/PP nanocomposite.

CONCLUSIONS

By analyzing XRD and TEM results, we have elucidated the dispersion of nanoclay particles in a PP matrix. Nanocomposites prepared by a solution technique and a subsequent melt-mixing process have numerous exfoliated platelets as well as intercalated platelets with increased d-spacing. The d-spacing value of C-15A in PP nanocomposites was found to be 3.651 nm. The number of intercalated layers in a single clay crystallite was determined to be 4, and the num-

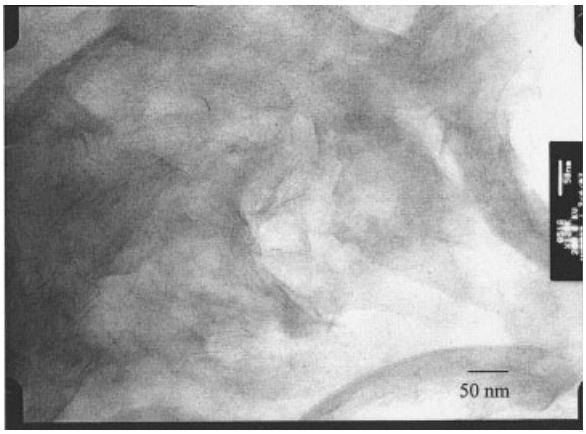

Figure 10 High-resolution TEM image of a C-15A/PP nanocomposite.

Figure 11 High-resolution TEM image of a C-15A/PP nanocomposite.

ber was confirmed by both XRD data and TEM images. The stage gallery structure has been modeled to show that the intercalant is a PP molecule. The stage gallery structure of montmorillonite particles in the nanocomposites has been determined according to the Daumas–Herold model, and it provides a molecular-level understanding of where the PP molecules might be intercalated within the available gallery spaces of the clay particles. A large number of clay platelets are exfoliated and dispersed uniformly in the polymer matrix, and this can be clearly concluded from the TEM images.

The authors are grateful to Steven B. Warner for his valuable technical discussions. They are also grateful to Southern Clay Products for a sample of organically modified montmorillonite clay.

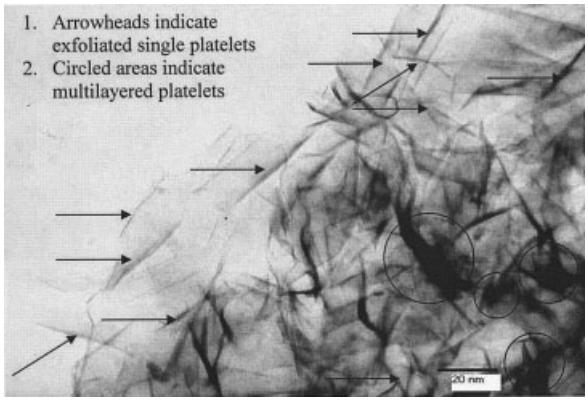

Figure 12 High-resolution TEM image of a C-15A/PP nanocomposite.

Figure 13 High-resolution TEM image of a C-15A/PP nanocomposite.

References

1. Kurauchi, T.; Okada, A.; Nomura, T.; Nishio, T.; Saegusa, S.; Deguchi, R. SAE Proceedings of International Congress and Exposition: Detroit, MI, 1991; Technical Paper Series No. 910584.
2. Giannelis, E. P. Adv Mater 1996, 8, 29.
3. Charles, E. The Chemistry of Clay Minerals; Elsevier: Amsterdam, 1973; p 20.
4. Van, H. O. An Introduction to Clay Colloid Chemistry; Wiley-Interscience: New York, 1991; Vol. 2, p 10.
5. Newman, A. C. D. Chemistry of Clays and Clay Minerals; Wiley: New York, 1987; p 20.
6. Theng, B. K. G. Chemistry of Clay–Organic Reactions; Wiley: New York, 1974; p 70.
7. Theng, B. K. G. Formation and Properties of Clay–Polymer Complexes; Elsevier: Amsterdam, 1979; p 65.
8. Destefani, J. D. Molding Syst 1999, 57, 10.
9. Michael, J. S.; Abdulwahab, S. A.; Kurt, F. S.; Anongnat, S.; Priya, V. Macromolecules 2001, 34, 1864.
10. Oya, A.; Kurokawa, Y. J Mater Sci 2002, 35, 1045.
11. Emmanuel, P. G. Adv Mater 1996, 8, 29.
12. Oh, W. C. Carbon Sci 2001, 2, 22.
13. Tanuma, S.; Kamimura, H. Graphite Intercalation Compounds; World Scientific: Philadelphia, 1985; p 30.
14. Zeng, C.; Lee, L. Proc ANTEC, SPE: San Francisco, 2002; p 2275.
15. Limin, L.; Zongneng, Q.; Xiaoguang, Z. J Appl Polym Sci 1999, 71, 1133.
16. Manias, E.; Touny, A.; Wu, L.; Lu, B.; Strawhecker, K.; Gilman, J. W.; Chung, T. C. Polym Mater Eng 2000, 82, 282.
17. Girish, G.; Ramesh, C.; Ashish, L. Macromolecules 2001, 34, 852.
18. Billmeyer, F. W. Textbook of Polymer Chemistry; Interscience: New York, 1957.
19. Warner, S. B. Fiber Science; Prentice Hall: Upper Saddle River, NJ, 1995.